Direct Preparation and Patterning of Iron Oxide Nanoparticles via Microcontact Printing on Silicon Wafers for the Growth of Single-Walled Carbon Nanotubes

Lei Ding, Weiwei Zhou, Haibin Chu, Zhong Jin, Yan Zhang, and Yan Li*

Beijing National Laboratory for Molecular Sciences, Key Laboratory for the Physics and Chemistry of Nanodevices, College of Chemistry and Molecular Engineering, Peking University, Beijing 100871, China

Received May 12, 2006. Revised Manuscript Received June 26, 2006

Direct fabrication of uniform patterns of $Fe_2O_3 \cdot xH_2O$ nanoparticles on the SiO_x/Si surface was achieved by microcontact printing (μCP). The as-prepared poly(dimethylsiloxane) (PDMS) stamps with a hydrophobic surface were used. The "ink" was an $FeCl_3 \cdot 6H_2O$ ethanol solution. $Fe_2O_3 \cdot xH_2O$ nanoparticles were formed on the stamps from the hydrolysis of $FeCl_3$ during the ink drying process and were then directly deposited onto the SiO_x/Si surface with μCP. The nanoparticles were transferred to the areas beneath the "raised" portions of the stamp at low ink concentration but populated at the areas beneath the "recessed" portions of the stamp at high ink concentration. The hydrophobic property of the stamp surface cooperated with the gravity of the particles in bringing on such an exchange of recession and repousse. The density and size of the formed nanoparticles could be tuned by varying the ink concentration. The patterned $Fe_2O_3 \cdot xH_2O$ nanoparticles were used as the catalysts for the growth of single-walled carbon nanotubes (SWCNTs) by CVD. By skillfully patterning the inks of different concentrations on the same SiO_x/Si wafer, we studied the effect of the ink concentration on the growth of SWCNTs. It is also shown that this simple method could be extended to the fabrication of other metal-containing nanoparticles.

I. Introduction

The size-tunable preparation[1] and patterning[2,3] of inorganic nanoparticles are of interest in many aspects. For example, various catalyst nanoparticles have been patterned on substrates and further used for the catalytic growth of nanomaterials.[4,5] Though many kinds of strategies have been developed for the preparation of nanoparticles and different techniques have been used to pattern them on substrates, it is still challenging to directly fabricate and pattern diameter-controlled nanoparticles on surfaces.

Microcontact printing (μCP) has been proven to be a powerful tool for the preparation of micro- to nanoscaled surface features over centimeter distances but requires no expensive facilities.[3,6] To date, it has been extended from patterning self-assembled monolayers (SAMs)[3] at the very beginning to patterning a variety of objects, such as biomolecules,[7] colloidal particles,[8] and polymers.[9] It has already been demonstrated that inorganic materials can be patterned with μCP.[10−13] However, the transfer of inorganic materials often relied on the assistance of polymers.[10] Very recently,

* To whom correspondence should be addressed, Tel: 86-10-62756773. E-mail: yanli@ pku.edu.cn.

(1) (a) Rotello, V. M. *Nanoparticles: Building Blocks for Nanotechnology*; Kluwer Academic/Plenum Publishers: New York, 2004; pp 1−27. (b) Cushing, B. L.; Kolesnichenko, V. L.; O'Connor, C. J. *Chem. Rev.* **2004**, *104*, 3893. (c) Suslick, K. S.; Price, G. J. *Annu. Rev. Mater. Sci.* **1999**, *29*, 295. (d) Pileni, M. P. *Langmuir* **1997**, *13*, 3266.

(2) (a) Xia, Y. N.; Whitesides, G. M. *Angew. Chem., Int. Ed.* **1998**, *37*, 551. (b) Qin, D.; Xia, Y.; Xu, B.; Yang, H.; Zhu, C.; Whitesides, G. M. *Adv. Mater.* **1999**, *11*, 1433.

(3) (a) Nyffenegger, R. M.; Penner, R. M. *Chem. Rev.* **1997**, *97*, 1195. (b) Gates, B. D.; Xu, Q.; Stewart, M.; Ryan, D.; Willson, C. G.; Whitesides, G. M. *Chem. Rev.* **2005**, *105*, 1171. (c) Love, J. C.; Estroff, L. A.; Kriebel, J. K.; Nuzzo, R. G.; Whitesides, G. M. *Chem. Rev.* **2005**, *105*, 1103. (d) Haryono, A.; Binder, W. H. *Small* **2006**, *2*, 600. (e) Chou, S. Y.; Krauss, P. R.; Renstrom, P. J. *Science* **1996**, *272*, 85. (f) Piner, R. D.; Zhu, J.; Xu, F.; Hong, S. H.; Mirkin, C. A. *Science* **1999**, *283*, 661. (g) Li, Q.; Zheng, J.; Liu, Z. *Langmuir* **2003**, *19*, 166.

(4) (a) Wang, D.; Tu, R.; Zhang, L.; Dai, H. *Angew. Chem., Int. Ed.* **2005**, *44*, 2925. (b) Yang, M.; Gracias, D. H.; Jacobs, P. W.; Somorjai, G. A. *Langmuir* **1998**, *14*, 1458.

(5) Javey, A.; Dai, H. *J. Am. Chem. Soc.* **2005**, *127*, 11942.

(6) (a) Renault, J. P.; Bernard, A.; Bietsch, A.; Michel, B.; Bosshard, H. R.; Delamarche, E.; Kreiter, M.; Hecht, B.; Wild, U. P. *J. Phys. Chem. B* **2003**, *107*, 703 (b) Li, H.; Kang, D.-J.; Blamire, M. G.; Huck, W. T. S. *Nano Lett.* **2002**, *2*, 347.

(7) (a) Bernard, A.; Renault, J. P.; Michel, B.; Bosshard, H. R.; Delamarche, E. *Adv. Mater.* **2000**, *12*, 1067. (b) Lange, S. A.; Benes, V.; Kern, D. P.; Hoerber, J. K. H.; Bernard, A. *Anal. Chem.* **2004**, *76*, 1641. (c) Renault, J. P.; Bernard, A.; Juncker, D.; Michel, B.; Bosshard, H. R.; Delamarche, E. *Angew. Chem., Int. Ed.* **2002**, *41*, 2320.

(8) (a) Hidber, P. C.; Helbig, W.; Kim, E.; Whitesides, G. M. *Langmuir* **1996**, *12*, 1375. (b) Santhanam, V.; Liu, J.; Agarwal, R.; Andres, R. P. *Langmuir* **2003**, *19*, 7881. (c) Cherniavskaya, O.; Adzic, A.; Knutson, C.; Gross, B. J.; Zang, L.; Liu, R.; Adams, D. M. *Langmuir* **2002**, *18*, 7029.

(9) (a) Choi, D.-G.; Yu, H. K.; Yang, S.-M. *Mater. Sci. Eng., C* **2004**, *24*, 213. (b) Wang, M.; Braun, H.-G.; Kratzmuller, T.; Meyer, E. *Adv. Mater.* **2001**, *13*, 1312. (c) Li, H.-W.; Muir, B. V. O.; Fichet, G.; Huck, W. T. S. *Langmuir* **2003**, *19*, 1963.

(10) (a) Wu, X. C.; Bittner, A. M.; Kern, K. *Adv. Mater.* **2004,** *16*, 413**.** (b) Wu, X. C.; Chi, L. F.; Fuchs, H. *Eur. J. Inorg. Chem.* **2005**, 3729. (c) Wang, Z.; Yuan, J.; Zhang, J.; Xing, R.; Yan, D.; Han, Y. *Adv. Mater.* **2003**, *15*, 1009.

(11) Zheng, Z.; Azzaroni, O.; Vickers, M. E.; Huck, T. S. *Adv. Mater.* **2006**, *16*, 805.

(12) Kind, H.; Bonard, J. M.; Emmenegger, C.; Nilsson, L. O.; Hernadi, K.; Maillard-Schaller, E.; Schlapbach, L.; Forro, L.; Kern, K. *Adv. Mater.* **1999**, *11*, 1285.

(13) (a) Kind, H.; Bonard, J.; Forró, L.; Kern, K.; Nilsson, L.; Schlapbach, L. *Langmuir* **2000**, *16*, 6877. (b) Gu, G.; Philipp, G.; Wu, X. C.; Burghard, M.; Bittner, A. M.; Roth, S. *Adv. Funct. Mater.* **2001**, *11*, 295.

10.1021/cm061122e CCC: $33.50
Published on Web 07/22/2006

Zheng et al.[11] reported the direct transfer of water-soluble inorganic salts with μCP. They used hydrophilic poly(dimethylsiloxane) (PDMS) stamps and modified the target substrate surfaces with SAMs to give them a higher affinity for the inorganic salts.

Uniform patterns of iron-containing nanoparticles on substrates with designed size are of interest because they can be used as the catalyst for chemical vapor deposition (CVD) growth of single-walled carbon nanotubes (SWCNTs).[15] μCP has been used to pattern iron-containing catalysts for the growth of carbon nanotubes (CNTs). For example, Kind et al. patterned $Fe(NO_3)_3$ ink on the surface that was used as the catalyst for the growth of multiwalled carbon nanotube (MWCNT) films.[12] μCP has also been applied to transfer Fe-containing gel-like catalyst precursors[13] or ferritin[14] for the growth of MWCNTs and SWCNTs. What we are interested in is the direct fabrication and uniform patterning of size-tunable $Fe_2O_3{\cdot}xH_2O$ nanoparticles on the SiO_x/Si surface with μCP. However, this has not been studied in the above literature. Our method needs neither surface treatment of the stamps nor modification of the substrates with SAMs. Moreover, the μCP technique allowed us to pattern nanoparticles with diverse sizes at different locations on one small piece of silicon wafer, which is very convenient in the experiment for the determination of optimum conditions for CVD growth of SWCNTs. Our results show that μCP can be widely used as a convenient tool for the preparation and patterning of some metal oxide particles.

II. Experimental Section

Materials. All chemicals used are of analytical grade. Water of Milli-Q quality obtained from the commercially available water purification equipment from Millipore (Bedford, MA) was used throughout the experiment. p-Type Si(111) wafers were cut into 1.0 cm × 1.0 cm pieces. After being ultrasonicated with ethanol and water for 5 min each and rinsed with water, the wafers were cleaned in piranha solution (H_2SO_4/H_2O_2 = 7/3, v/v) at 100 °C for 30 min, rinsed with water, and blown dry with high-purity nitrogen. The wafer was then dipped in 5% HF solution and rinsed with water. At last, the wafer was mounted in the furnace at 950 °C for 2.5 h to obtain the SiO_x/Si surface. The as-prepared PDMS stamps were used with no further treatment except for cleaning with water and ethanol.

Inking and Printing. Our procedures for the synthesis of $Fe_2O_3{\cdot}xH_2O$ nanoparticles on the SiO_x/Si surface with μCP for the growth of SWCNTs are shown in Scheme 1. The ink for the μCP was an $FeCl_3{\cdot}6H_2O$ ethanol solution. The ink was applied to the stamp by covering the stamp with the ink solution using a pipet and then dried under atmospheric conditions. The ink was then transferred onto the surface of the silicon wafer by bringing the stamp into conformal contact with the substrate for 5 min. After being peeled off by hand, the surface of the substrate was examined with an optical microscope.

Scheme 1. Schematic Illustration of the Procedures for the Preparation and Patterning of $Fe_2O_3{\cdot}xH_2O$ Nanoparticles and the Growth of SWCNTs on SiO_x/Si Surface

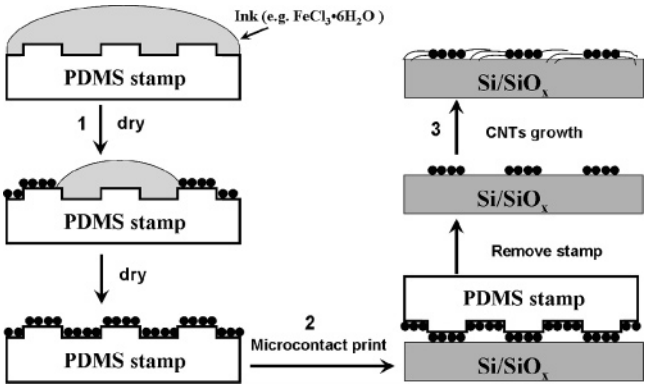

Step 1: "Ink" the stamp with the $FeCl_3{\cdot}6H_2O$ ethanol solution using a pipette and dry under atmosphere conditions. Step 2: Bring the stamp into conformal contact with the substrate for 5 min, and the formed $Fe_2O_3{\cdot}xH_2O$ nanoparticles transfer onto the silicon oxide substrate; remove the stamp, and a patterned array of $Fe_2O_3{\cdot}xH_2O$ nanoparticles then forms on the surfaces. Step 3: The SiO_x/Si wafer is put into a tube reactor and the CVD growth of SWCNTs proceeds.

Growth of SWCNTs. The CVD growth of SWCNTs was performed in procedure similar to that in our previous paper.[16] The wafer was put into a horizontal quartz tube furnace equipped and calcined in air at 700 °C for 5 min, and then heated to 900 °C in Ar and reduced in H_2 (220 sccm) for 5 min. Subsequently, CVD growth of SWCNTs proceeded at 900 °C with CH_4 (800 sccm) as the feeding gas for 15 min, followed by cooling the furnace in Ar to room temperature. The direction of gas flow was parallel to the line patterns of the catalyst on the substrate.

Characterization. A SPI3800 scanning probe microscope (SPM, Seiko Instrument Inc.) equipped with a 100 μm scanner was used for AFM imaging, and all topographic images were recorded with tapping-mode (TM) AFM. Scanning electron microscope (SEM, FEIXL30 S−FEG, operated at 1 kV) and micro-Raman spectroscope (Renishaw 2000) were used to characterize the produced nanoparticles and SWCNTs. The excitation wavelength of the micro-Raman is 514.5 nm sourced by an Ar ion laser.

III. Results and Discussion

Formation of $Fe_2O_3{\cdot}xH_2O$ Nanoparticle Patterns. The typical images we got by μCP are shown in Figure 1. The SEM images in images A and B of Figure 1 and the optical image in Figure 1D show that well-organized structures can be fabricated. The TM-AFM images in Figure 1C−F show that the edges of the patterns are very sharp and no diffusion occurred at the recessed portion of the stamp. The mean thickness of the nanoparticle films in Figure 1A−C is 18 nm. The mean diameter of the nanoparticles in Figure 1D−F is 10 nm.

The nanoparticles transferred onto the silicon wafers were characterized with EDX and XRD (panels G and H of Figure 1). It was found from the EDX spectrum that little Cl element exists in the samples. And all the peaks in the XRD pattern can be readily addressed to $Fe(OH)_3$ (JCPDS 38-0032), orthorhombic $Fe(OH)_3$ (JCPDS 46-1436), and β-$Fe_2O_3{\cdot}nH_2O$ (JCPDS 08-0093), which are generally denoted as $Fe_2O_3{\cdot}$

(14) Bonard, J.-M.; Chauvin, P.; Klinke, C. *Nano Lett.* **2002**, *2*, 665.
(15) (a) Li, Y.; Liu, J.; Wang, Y. Q.; Wang, Z. L. *Chem. Mater.* **2001**, *13*, 1008. (b) An, L.; Owens, J. M.; McNeil, L. E.; Liu, J. *J. Am. Chem. Soc.* **2002**, *124*, 13688. (c) Fu, Q.; Huang, S.; Liu, J. *J. Phys. Chem. B* **2004**, *108*, 6124. (d) Li, Y.; Kim, W.; Zhang, Y.; Rolandi, M.; Wang, D.; Dai, H. *J. Phys. Chem. B* **2001**, *105*, 11424.
(16) Zhou, W.; Zhang, Y.; Li, X.; Yuan, S.; Jin, Z.; Xu, J.; Li, Y. *J. Phys. Chem. B* **2005**, *109*, 6963.

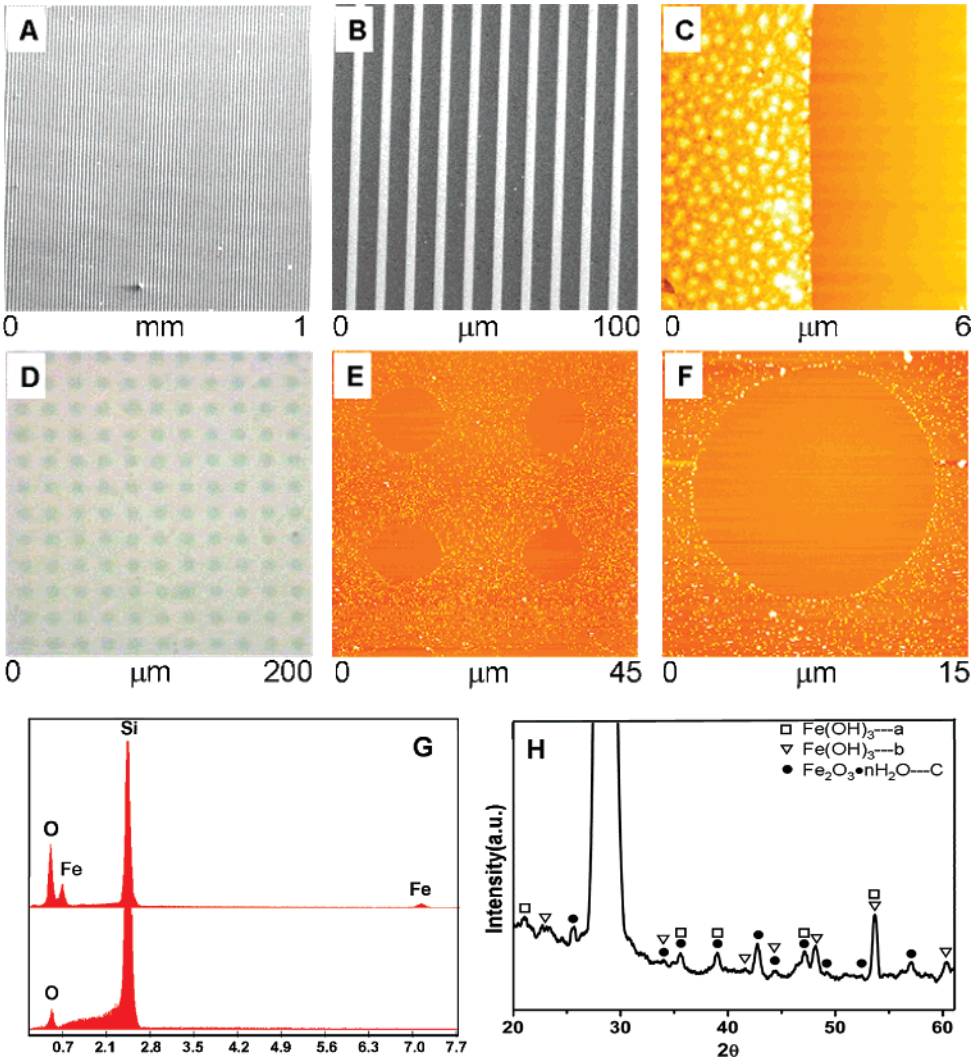

Figure 1. Line-shaped (A−C) and mesh-shaped (E−F) patterns of nanoparticles fabricated by μCP with ink concentrations of 0.5 mM and 0.2 mM, respectively, and the corresponding EDS (G) and XRD (H) characterization results. A and B are SEM images. D is an optical image. C−F are TM-AFM topographic images. The upper plot in (G) was the measurement on the patterned area and the lower one was the measurement on the positions without nanoparticles.

xH_2O hereafter. These results hint that the $FeCl_3 \cdot 6H_2O$ hydrolyzed completely and produced $Fe_2O_3 \cdot xH_2O$ when the ink was applied onto the stamp and dried. The crystal water in $FeCl_3 \cdot 6H_2O$ and the condensed water from air acted as the water sources. Along with the evaporation of ethanol, the concentration of water increased and hydrolysis took place. The hydrolysis was further driven by the volatilization of the produced HCl until $FeCl_3$ was hydrolyzed thoroughly. Kern et al. reported a similar mechanism when they used $Fe(NO_3)_3 \cdot 9H_2O$ ethanol solution as the ink.[12] When the ink concentration was higher (here 0.5 mM), more $Fe_2O_3 \cdot xH_2O$ formed on the stamp and nanoparticle films were transferred onto the silicon wafer (Figure 1A−C). When the ink was much diluted (here 0.2 mM), less $Fe_2O_3 \cdot xH_2O$ formed and well-dispersed nanoparticles were transferred onto the surface.

The μCP was initially used to form patterns of organic molecule SAMs on the substrate.[3] Recently, the direct patterning of various materials with μCP has been focused on for its designable, simple, and cleanly procedures. Yet compared to the patterning of SAMs, such a process is more complicated. This is partially due to the difficulty in finding compatible stamp−molecule−substrate systems.[10] It is essential that the target molecules are more affinitive to surface of the substrate than to that of the stamp. When the PDMS stamps were treated by O_2 plasma, as is usually done,[11] the surfaces of the stamps became highly polar and hydrophilic. This kind of stamp is suitable for the printing of organic molecules because the molecules are more affinitive to the less-polar substrates. When they are used for printing inorganic molecules, the surface of the substrate must be modified with SAM to gain a higher affinity with the target molecules.[11] The stamps here were used with no plasma treatment, and the surfaces were hydrophobic. This kind of surface has a low affinity with inorganic materials, which is in favor of the direct delivering of $Fe_2O_3 \cdot xH_2O$ nanoparticles to the more hydrophilic substrates of silicon wafers.

Considering the surface affinity, it seems that this should be a general method for the direct patterning of many kinds of metal oxides. Our further experiments give more evidence about this, as shown in the Supporting Information.

Effects of Ink Concentration on the Formation of $Fe_2O_3 \cdot xH_2O$ Nanoparticles. The concentration of ink is always an important factor in the μCP process. When the

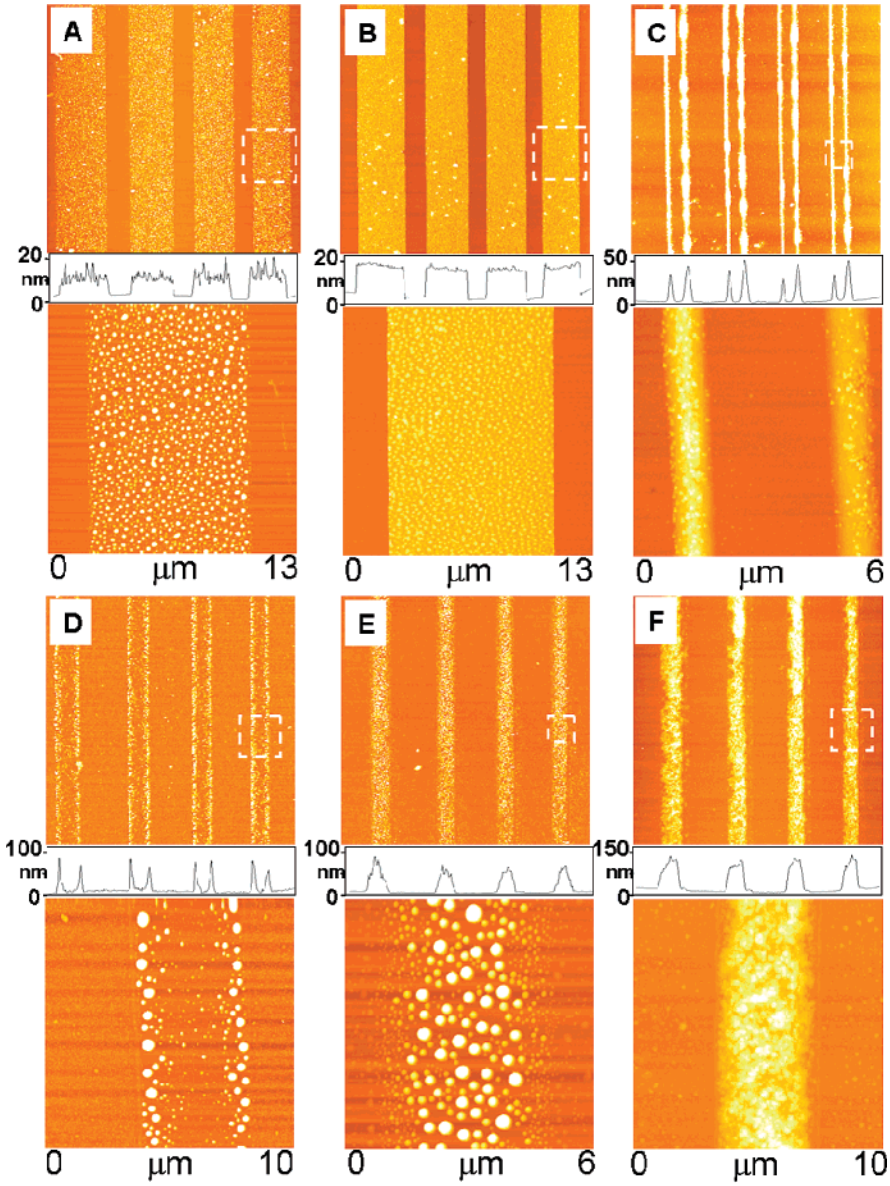

Figure 2. AFM topographic images of nanoparticle patterns fabricated with different ink concentrations of (A) 0.2, (B) 0.5, (C) 2.0, (D) 5.0, (E) 10.0, and (F) 20.0 mM. Each upper image is the AFM image of lower magnification with scanning area of 45 × 45 μm; each middle picture is the cross-section profile of the lower magnification; each nether image is the AFM image of higher magnification amplified from the area marked in the corresponding lower-magnification image.

concentration of $FeCl_3 \cdot 6H_2O$ ethanol solution was systematically changed, dramatic changes in the diameters and populations of the nanoparticles were observed (Figure 2). Individual nanoparticles with a mean diameter of about 20 nm formed on the SiO_x/Si surface when the ink concentration was 0.2 mM. The mean thickness of the sparse film is about 10 nm. (Figure 2A). A relative compact film with a thickness of about 18 nm formed when the concentration was 0.5 mM (Figure 2B). But when the concentration was increased to 2.0 mM, the population of the nanoparticles formed on the raised portions of the stamp decreased and most of the nanoparticles condensed on the edges of the recessed portion (Figure 2C). When the concentration was increased to 5.0 mM, nanoparticles started to condense on the area beneath the recessed portions of the stamp (Figure 2D). The features became higher when the concentration was further increased (images E and F of Figure 2). And along with the increase in ink concentration, the formed particles in the patterns grew larger, as shown in the AFM images of higher magnification in Figure 2.

It can be found from the above that the $Fe_2O_3 \cdot xH_2O$ nanoparticles tend to stay on the areas of the substrates beneath the raised portions of the stamp at low ink concentration; yet at high ink concentration, more nanoparticles tend to condense on the areas beneath the recessed portions of the stamp. The surface properties of the stamps we used contributed much to this phenomenon of the exchange of recession and repousse. As ethanol could wet the PDMS very well, the ink solution spread along the stamp and formed a smooth outer surface when it was dropped on the stamp. Relatively more ink solution then filled in the recessed portion of the stamp; therefore, more particles were formed during the ink drying process. At low concentration, very tiny nanoparticles formed on both the raised and the recessed portions of the stamp. When the stamp was brought into contact with the SiO_x/Si surface, only the nanoparticles

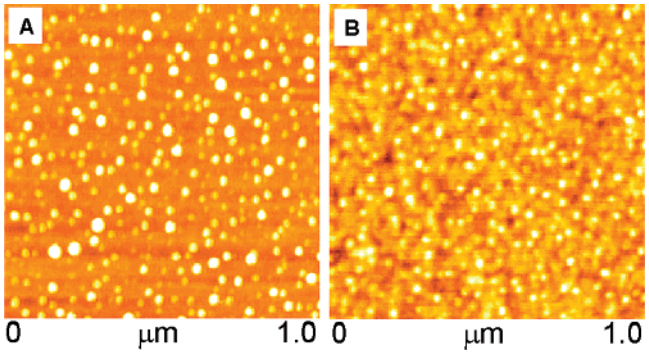

Figure 3. AFM topographic images of the as prepared Fe_2O_3·xH_2O nanoparticles (from 1.0 mM ink) on (A) the SiO_x/Si surface and (B) those nanoparticles after being calcined at 350 °C for 1 h under atmospheric conditions.

on the raised portion of the stamp were transferred onto the SiO_x/Si surface. But when the ink concentration was very high, more nanoparticles with larger sizes formed at the recessed portions of the stamp. As the stamps we used are hydrophobic, the interaction between the particles and the stamp surface should be very weak. This enhanced the aggregation of particles. Along with the size increase of the particles, the factor of the particles' gravity becomes important and inevitable. When the stamp was brought into contact with the SiO_x/Si surface, the particles in the recessed portion of the stamp moved onto the surface driven by gravity.

CVD Growth of SWCNTs. In the experiment, it was found that the volume of the ink applied on the stamp by the pipet could affect the dispersing of the nanoparticles. To fabricate patterns of well-dispersed individual Fe_2O_3·xH_2O nanoparticles on the SiO_x/Si surface, much less ink (only 2 μL here) has been applied onto the stamp. The AFM image of the produced nanoparticles is shown in Figure 3. One hundred nanoparticles were individually measured from the height profiles using AFM. It was found that the size distribution was narrow, and the average diameter of the nanoparticles was 3.9 nm. After being calcined at 350 °C for 1 h under atmospheric conditions, the average diameter of the nanoparticles changed to 0.9 nm (Figure 3B).

Using the produced iron oxide nanoparticles as catalysts, we grew SWCNTs at a high yield via the CVD process, as shown in Figure 4. The Raman spectrum shows that the CNTs on the SiO_x/Si surface are single-walled ones.

Scheme 2. Schematic Illustration of the Procedures for the Arrayed Synthesis of Fe_2O_3·xH_2O Nanoparticles with Different Ink Concentrations by μCP and the Growth of SWCNTs

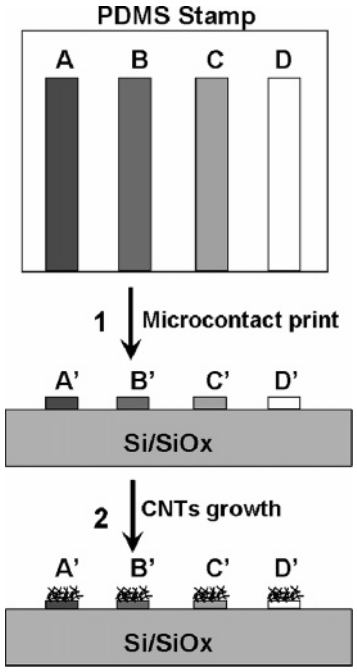

Step 1: Apply 1 μL of ink by pipette at the edge of the PDMS stamp; the drop of ink spreads along the line pattern of the stamp and forms a tangle-shaped area A that is about 0.8 mm in width. Tangle-shaped areas B−D are then inked in turn by the same method with inks of different concentration. After being dried, the modified stamp is brought into contact with the SiO_x/Si surface for μCP. As a result, four areas with different densities of Fe_2O_3·xH_2O nanoparticles are fabricated. Step 2: The SiO_x/Si wafer is put into a tube reactor, and the CVD growth of SWCNTs proceeds.

We also studied the effect of ink concentration on the growth of SWCNTs by patterning the inks of different concentration on one piece of SiO_x/Si wafer. Scheme 2 outlines the procedures. First, different areas (each with a width of 0.8 mm and length of 8.0 mm) of the stamp were inked with $FeCl_3$·$6H_2O$ alcohol solutions of diverse concentrations by pipets. After being dried, the stamp was brought into contact with the SiO_x/Si surface for μCP. As a result, each area of the wafer was occupied by iron oxide nano-

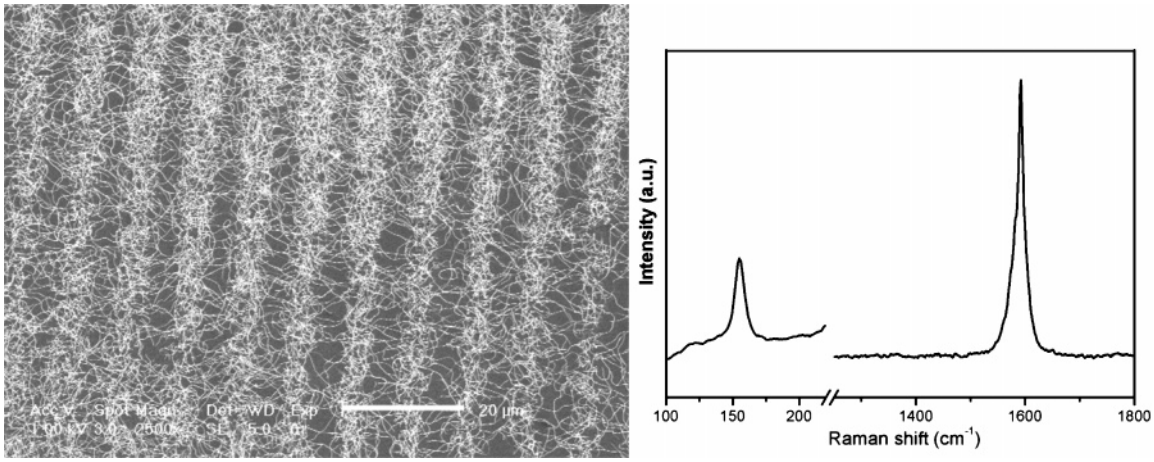

Figure 4. SEM image and Raman characterization of SWCNTs grown from the fabricated Fe_2O_3·xH_2O nanoparticles on the SiO_x/Si surface by CVD; 1.0 mM $FeCl_3$·$6H_2O$ ethanol solution was used as the ink for μCP, scale bar = 20 μm.

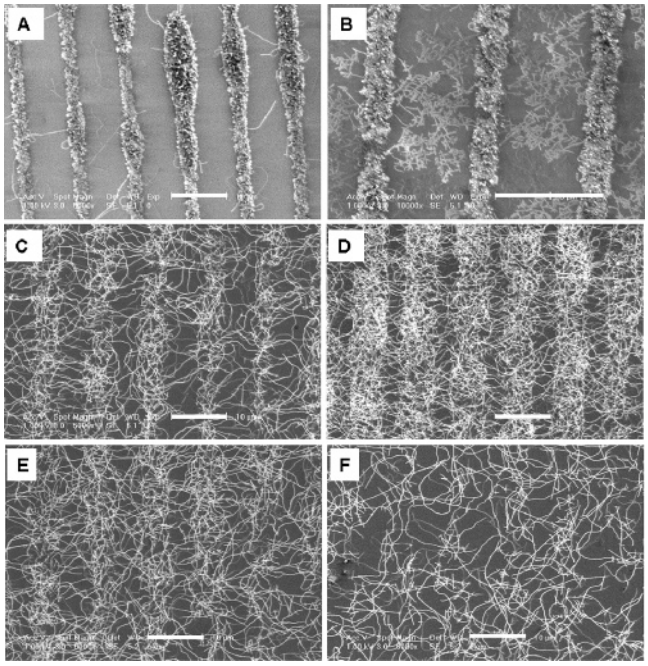

Figure 5. Dependence of the growth of SWCNTs on the concentration of the printed catalyst: (A) 20.0, (B) 10.0, (C) 2.0, (D) 0.5, (E) 0.2, and (F) 0.1 mM; scale bar = 10 μm.

particles of different diameter and population. The wafer was then mounted in the tube reactor and the CVD process proceeded. Figure 5 shows the experimental results. When the ink concentration was 20 mM, very few CNTs were formed on the surface (Figure 5A). This is because that the particles fabricated under high ink concentrations were too big to grow SWCNTs. When the concentration was reduced to 10 mM, some relatively short CNTs were formed (Figure 5B). The high yield of SWCNTs grew from the areas inked by $FeCl_3$ with concentrations of 2.0, 0.5, and 0.2 mM (Figure 5C−E). The density of SWCNTs decreased when the ink concentration was down to 0.1 mM. All of the results came from one stamp and one piece of SiO_x/Si wafer, so we can guarantee the identity of both the μCP and the CVD processes.

We extended the μCP method to the $NiCl_2 \cdot 6H_2O$ system. The fabricated Ni-containing nanoparticles on the SiO_x/Si surface were used to grow MWCNTs by CVD (see the Supporting Information).

IV. Conclusions

Using hydrophobic PDMS as stamp, we directly patterned uniform patterns of $Fe_2O_3 \cdot xH_2O$ nanoparticles, which formed during the ink drying process, on the SiO_x/Si surface by μCP. The low affinity of the hydrophobic stamp with $Fe_2O_3 \cdot xH_2O$ nanoparticles was thought to be crucial for directly patterning. As an important factor in the μCP process, the effect of ink concentration was studied. The exchange of recession and repousse phenomenon was observed at high ink concentrations, in which the aggregation of nanoparticles and gravity were regarded as the driving forces. Using the fabricated $Fe_2O_3 \cdot xH_2O$ nanoparticles as catalysts, we grew SWCNTs in high yield by the thermal CVD method on the SiO_x/Si surface. We also studied the effect of the ink concentration on the growth of SWCNTs by patterning the inks of different concentration on the same SiO_x/Si wafer. We extend the method to fabricate other metal oxides such as Ni-containing nanoparticles. We think this simple method may be adaptable to more metal and semiconductor oxides or hydroxides, which will open a door to fields from catalyst patterning to nanodevice fabrication. Further research is underway in our lab.

Acknowledgment. This work was supported by the NSF (Project 90406018), MOST (Project 2001CB610501), and MOE of China.

Supporting Information Available: Additional AFM and SEM images from further experiments. This material is available free of charge via the Internet at http://pubs.acs.org.

CM061122E